Flavin and Heme Structures in Lactate:Cytochrome *c* Oxidoreductase: A Resonance Raman Study†

Alain Desbois,*,‡ Mariella Tegoni,§ Michel Gervais,§ and Marc Lutz‖

Laboratoire de Biophysique, Institut de Biologie Physico-Chimique, 13 Rue Pierre et Marie Curie, 75005 Paris, France, Laboratoire d'Enzymologie Physico-Chimique, Centre de Génétique Moléculaire du CNRS, Laboratoire propre du CNRS associé à l'Université Pierre et Marie Curie, 91190 Gif-sur-Yvette, France, and Service de Biophysique, Département de Biologie du Centre d'Etudes Nucléaires de Saclay, 91191 Gif-sur-Yvette Cedex, France

Received February 16, 1989; Revised Manuscript Received May 16, 1989

ABSTRACT: Resonance Raman spectra of *Hansenula anomala* L-lactate:cytochrome *c* oxidoreductase (or flavocytochrome b_2), of its cytochrome b_2 core, and of a bis(imidazole) iron–protoporphyrin complex were obtained at the Soret preresonance from the oxidized and reduced forms. Raman contributions from both the isoalloxazine ring of flavin mononucleotide (FMN) and the heme b_2 were observed in the spectra of oxidized flavocytochrome b_2. Raman diagrams showing frequency differences of selected FMN modes between aqueous and proteic environments were drawn for various flavoproteins. These diagrams were closely similar for flavocytochrome b_2 and for flavodoxins. This showed that the FMN structure must be very similar in both types of proteins, despite their very different proteic pockets. However, the electron density at this macrocycle was found to be higher in flavocytochrome b_2 than in these electron transferases. No significant difference was observed between the heme structures in flavocytochrome b_2 and in cytochrome b_2 core. The porphyrin center–N(pyrrole) distances in the oxidized and reduced heme b_2 were estimated to be 1.990 and 2.022 Å from frequencies of porphyrin skeletal modes, respectively. The frequency of the vinyl stretching mode of protoporphyrin was found to be very affected in resonance Raman spectra of flavocytochrome b_2 and of cytochrome b_2 core (1634–1636 cm^{-1}) relative to those observed in the spectra of iron–protoporphyrin [bis(imidazole)] complexes (1620 cm^{-1}). These specificities were interpreted as reflecting a near coplanarity of the vinyl groups of heme b_2 with the pyrrole rings to which they are attached. The low-frequency regions of resonance Raman indicated that the iron atoms of the four hemes b_2 are in the porphyrin plane whatever their oxidation state. The histidine–Fe–histidine symmetric stretching mode was located at 205 cm^{-1} in the spectra of flavocytochrome b_2 and of cytochrome b_2 core. It was insensitive to the iron oxidation state and indicated strong Fe–His bonds in both states.

L-Lactate:cytochrome *c* oxidoreductase (EC 1.1.2.3) or flavocytochrome b_2 (flavocyt b_2)[1] is a tetrameric enzyme. Each protomer contains one iron(III)–protoporphyrin IX ($Fe^{III}PP$) and one flavin mononucleotide (FMN) (Appleby & Morton, 1959). This mitochondrial enzyme has been purified from several yeasts (*Saccharomyces cerevisiae* and *Hansenula anomala*) and is a component of the following respiratory chain (Pajot & Claisse, 1974):

L-(+)-lactate → flavocyt b_2 → cyt *c* → cyt *a* + a_3 → O_2

The FMN group is the primary acceptor of the two electrons donated by L-lactate. This step is followed by a rapid one-electron transfer from the flavin to the heme b_2 group, which itself gives one electron to ferricytochrome *c* (Labeyrie, 1982). This reduction occurs within a "flavocytochrome b_2/cytochrome *c* complex" (Capeillère-Blandin, 1982; Tegoni et al., 1983).

Each protomer of flavocyt b_2 is folded up into two functional domains (Gervais et al., 1977, 1983; Celerier et al., 1989): a flavodehydrogenase domain and a cytochrome domain or cytochrome b_2 "core", which is homologous in sequence to microsomal cytochrome b_5 (Guiard et al., 1974; Haumont et al., 1987). These two domains are linked through one protease-sensitive segment (Gervais et al., 1977).

A full understanding of the molecular mechanism of electron transfer in flavocyt b_2 requires detailed information concerning the structures and environments of chromophores. A three-dimensional structure of flavocyt b_2 from bakers' yeast has been recently determined (Xia et al., 1987; Mathews & Xia, 1987). However, the 2.4–3.0-Å resolution of this structure does not yet yield detailed structural information on the chromophores at the atomic level. Moreover, this crystal structure displays the enzyme in two distinct states likely arising from crystal packing forces. In order to gain an insight into the heme and flavin structures occurring in flavocyt b_2, we have therefore studied the resonance Raman (RR) spectra of this enzyme, of its cytochrome b_2 core, and of a *b*-type heme model compound simulating the coordination properties of heme b_2. Resonance Raman spectroscopy indeed has been yielding considerable knowledge about structures and interactions of hemes and flavins in hemoproteins and flavoproteins (Spiro, 1985; Kitagawa & Ozaki, 1987; Müller, 1981; Müller

† Supported, in part, by grants from the Centre National de la Recherche Scientifique (URA 119 and UPR 319) and by grants from the Institut National de la Santé et de la Recherche Médicale (CRE 861012).

* Author to whom correspondence should be addressed.
‡ Institut de Biologie Physico-Chimique, Paris.
§ Centre de Génétique Moléculaire, Gif-sur-Yvette.
‖ Centre d'Etudes Nucléaires, Saclay.

[1] Abbreviations: flavocyt b_2, flavocytochrome b_2; cyt b_2, cytochrome b_2 core; cyt *c*, cytochrome *c*; PP, protoporphyrin IX; ImH, imidazole; 1MeIm, 1-methylimidazole; FMN, flavin mononucleotide; FAD, flavin adenine dinucleotide; CTABr, cetyltrimethylammonium bromide; RR, resonance Raman; PED, potential energy distribution.

0006-2960/89/0428-8011$01.50/0

et al., 1983; Morris & Bienstock, 1986). A preliminary account of this work has been given by Desbois et al. (1988). Finally, we have measured the effect of flavocyt b_2/cytochrome c complexation on the RR spectra of hemes b and c.

Experimental Procedures

Protein Preparations. Flavocytochrome b_2 from *Hansenula anomala* yeast was purified and characterized by methods previously described (Labeyrie et al., 1978; Gervais et al., 1980). The enzyme was precipitated with 50% saturation of ammonium sulfate in 100 mM sodium D,L-lactate and 100 mM Na,K_2PO_4 buffer, pH 7.0, and stored at 4 °C. Flavocyt b_2 concentration was determined spectrophotometrically on the reduced form, in the presence of D,L-lactate or sodium dithionite, with an extinction coefficient of 183 $mM^{-1}\cdot cm^{-1}$ at 423 nm (Pajot & Groudinsky, 1970).

Cytochrome b_2 core (cyt b_2) was prepared from *H. anomala* flavocyt b_2 by controlled trypsinolysis as described by Gervais et al. (1977) and Silvestrini et al. (1986). Its concentration was determined on the dithionite-reduced form with an extinction coefficient of 179 $mM^{-1}\cdot cm^{-1}$ at 423 nm. Cyt b_2 core was precipitated at 85% saturation of ammonium sulfate in 100 mM sodium D,L-lactate and 100 mM Na,K_2PO_4 buffer, pH 7.0, and stored at 4 °C.

In order to remove the D,L-lactate and ammonium sulfate for the Raman experiments, the dissolved enzyme or dissolved cyt b_2 core was dialyzed several times against a 10 mM phosphate buffer, pH 7.0, or a 20 mM phosphate buffer, pH 7.3.

Horse heart cytochrome c (Sigma, type VI) was completely oxidized by a slight excess of ferricyanide and purified by gel filtration through Sephadex G-50 equilibrated with 10 mM phosphate buffer, pH 7.0. The concentration of cyt c was determined spectrophotometrically with data from Schejter et al. (1963).

Bis(imidazole) Complex of Iron–Protoporphyrin. Protohemin chloride (Sigma, type I) was used without further purification and dissolved in an aqueous sodium hydroxide solution (ca. 10 mM). The bis(imidazole) complex of iron (III)–protoporphyrin ($Fe^{III}PP$) was formed by addition of imidazole (ImH) at a final concentration of 0.85–1.0 M. In order to avoid problems of aggregation due to these high ligand concentrations, the solutions were prepared in the presence of cetyltrimethylammonium bromide (CTABr) at a final concentration of 2% (w/v). The reduction of $Fe^{III}PP(ImH)_2$ was obtained by addition under vacuum of solid dithionite (~4 M excess) contained in a side arm of the Raman cell (Desbois & Lutz, 1981).

Spectroscopy. Resonance Raman spectra were obtained with 441.6-nm excitation from a helium–cadmium laser (Liconix Model 4050) and recorded at room temperature on a Jobin Yvon spectrometer (Ramanor HG25-UV). Grazing incidence of the excitation laser beam was used (Desbois et al., 1979). The signal to noise ratios were improved by summation of individual spectra in a multichannel analyzer (Tracor Northern TW1710).

After a long time of laser irradiation (≥20 min) on samples of oxidized flavocyt b_2, the RR spectra exhibited slight alterations. Taking into account the high-frequency regions of these spectra (1300–1700 cm^{-1}), these spectral modifications were attributed to a slow formation of reduced hemes b_2. This reduction may be indirect, mediated by a photoreduction of the bound FMN or of traces of free FMN (Kitagawa et al., 1980). Alternatively, a direct heme photoreduction may be considered as in the case of methemoglobin (Kitagawa & Nagai, 1979). The mechanism of the light-induced reduction of hemes b_2 was not investigated. However, we observed that the enzyme entirely recovered its oxidized state after laser illumination was stopped. Therefore, scans were interspersed with a short time (~1 min) of darkness on the sample during the accumulation of the RR signal. Under these conditions, the ferroheme contribution in the RR spectra of oxidized flavocyt b_2 was found to be negligible. On the other hand, we noted that the oxidized cyt b_2 core is not photoreducible under the same conditions of irradiation.

In the cases where the RR spectra were obtained on a fluorescence background the Raman spectrum was extracted from the total signal by a computer subtraction.

The spectrophotometric measurements were made with Cary 118C or Beckman DU7 spectrophotometers.

Results

Oxidized Forms of Flavocytochrome b_2, Cytochrome b_2 Core, and $FePP(ImH)_2$

Higher Frequency Regions (1000–1650 cm^{-1}). The high-frequency regions of RR spectra of flavocyt b_2(III), cyt b_2 core [cyt b_2(III)], and $Fe^{III}PP(ImH)_2$, excited at 441.6 nm, are displayed in Figure 1. Comparison of these spectra shows that flavocyt b_2(III) exhibits RR bands from both FMN and hemes b_2. Low-spin ferric complexes of protoheme indeed are not expected to yield any strong Raman bands at 1360 and 1408 cm^{-1} while FMN in water produces strong bands at 1355 and 1412 cm^{-1} when excited in the visible region (Nishimura & Tsuboi, 1978; Benecky et al., 1979; Irwin et al., 1980; Copeland & Spiro, 1986). Conversely, the strong 1374-cm^{-1} band is characteristic of low-spin ferriprotohemes (Spiro, 1985; Kitagawa & Ozaki, 1987) (Figure 1B,C). Taking the intensity of the 1374-cm^{-1} band as an internal standard, we have subtracted the spectrum of the cyt b_2 core from that of flavocyt b_2. The difference spectrum (Figure 1D) exhibits bands at 1067, 1085, 1131, 1165, 1180, 1231, 1257, 1284, 1302, 1360, 1408, 1463, 1501, 1557, 1581, and 1629 cm^{-1}, i.e., at frequencies close to those observed for FMN in water, except for the 1085-cm^{-1} band, for which no homologous band is observed with 465–600-nm excitations (Nishimura & Tsuboi, 1978; Benecki et al., 1979; Irwin et al., 1980; Copeland & Spiro, 1986). However, RR spectra of lumiflavin in water excited at 488 nm clearly exhibit this band at 1085 cm^{-1} (Nishina et al., 1980). Therefore, although the relative intensities and frequencies of heme bands may not necessarily be exactly identical in RR spectra of flavocyt b_2(III) and of cyt b_2(III), all the preceding frequencies are assigned to flavin modes of FMN bound to flavocyt b_2(III) (Table I).

The 1374-cm^{-1} band corresponds to the ν_4 mode of Fe(III)–porphyrin according to the nomenclature of Abe et al. (1978). Its frequency is the same in RR spectra of the hemoproteins (Figure 1). The porphyrin core size marker frequencies (ν_3, ν_{38}, ν_2, ν_{37}, and ν_{10}) are clearly observed at 1505, 1557, 1579, 1598, and 1640 cm^{-1} in spectra of both flavocyt b_2(III) and cyt b_2(III). None of them differs by more than 3 cm^{-1} from these of $Fe^{III}PP(ImH)_2$ (Figure 1). As far as the frequencies of vinyl modes are concerned, only the 1620-cm^{-1} band of $Fe^{III}PP(ImH)_2$ appears to be strongly affected in the spectra of the hemoproteins (1634 and 1636 cm^{-1}) (Figure 1).

Medium-Frequency Regions (450–1000 cm^{-1}). Comparison of spectra A and B of Figure 2 shows that bands observed at 839, 785, 751, 640, 610, 525, and 454 cm^{-1} are attributable to FMN modes of flavocyt b_2(III).

Two bands located at 480 and 501 cm^{-1} in RR spectra of $Fe^{III}PP(ImH)_2$ (Figure 2C) are upshifted at ~491 and 541 cm^{-1} in those of cyt b_2(III) and of flavocyt b_2(III) (Figure

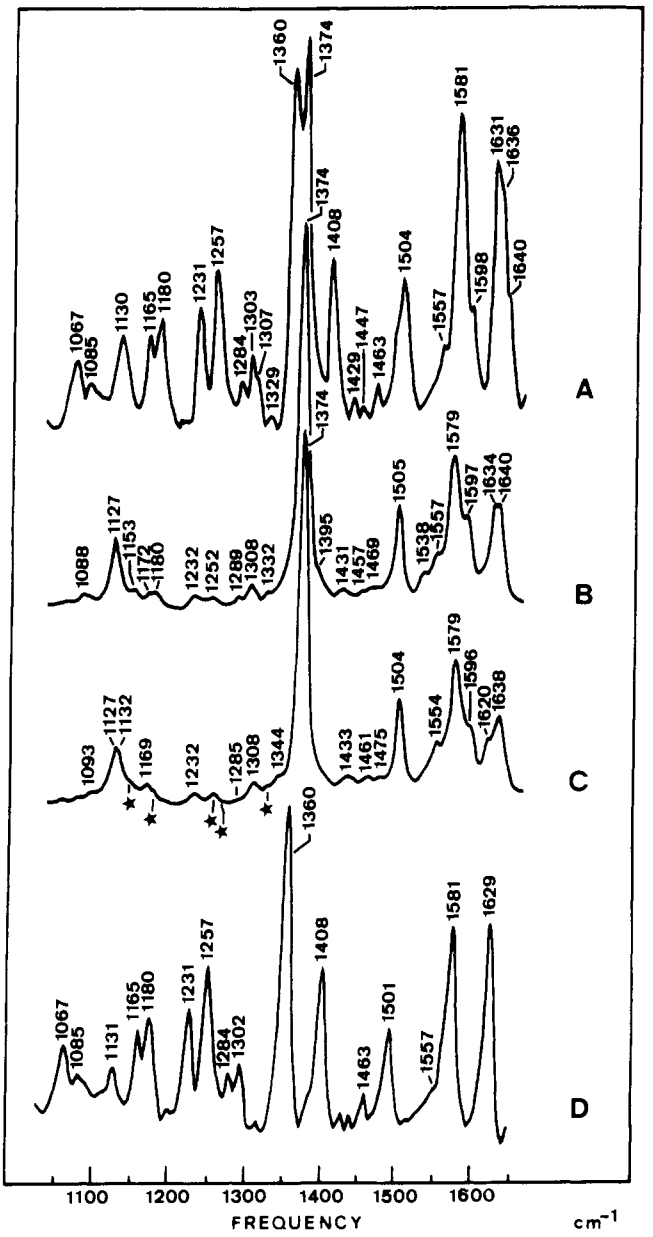

FIGURE 1: High-frequency regions (1050–1650 cm^{-1}) of resonance Raman spectra of oxidized flavocytochrome b_2 (A), cytochrome b_2 core (B), and bis(imidazole) complex of ferriprotoporphyrin in 2% CTABr aqueous solution (C). Experimental conditions: excitation wavelength, 441.6 nm; laser power, 40 mW; scanning speed, 25 cm^{-1}·mm^{-1}; time constant, 5 s; summation from four to six scans. Protein concentration, 0.6 mM (heme concentration) in 10 mM phosphate buffer (pH 7.3); Fe–protoporphyrin concentration, 0.8 mM; imidazole concentration, 0.8 M. The bands marked with a star below spectrum C are due to excess imidazole; spectrum D = spectrum A − 0.8(spectrum B). Independent experiments indicated that the uncertainties on the frequencies of FMN bands of this difference spectrum were ±1 cm^{-1} except for the 1131- and 1501-cm^{-1} bands, for which they were ±2 cm^{-1}.

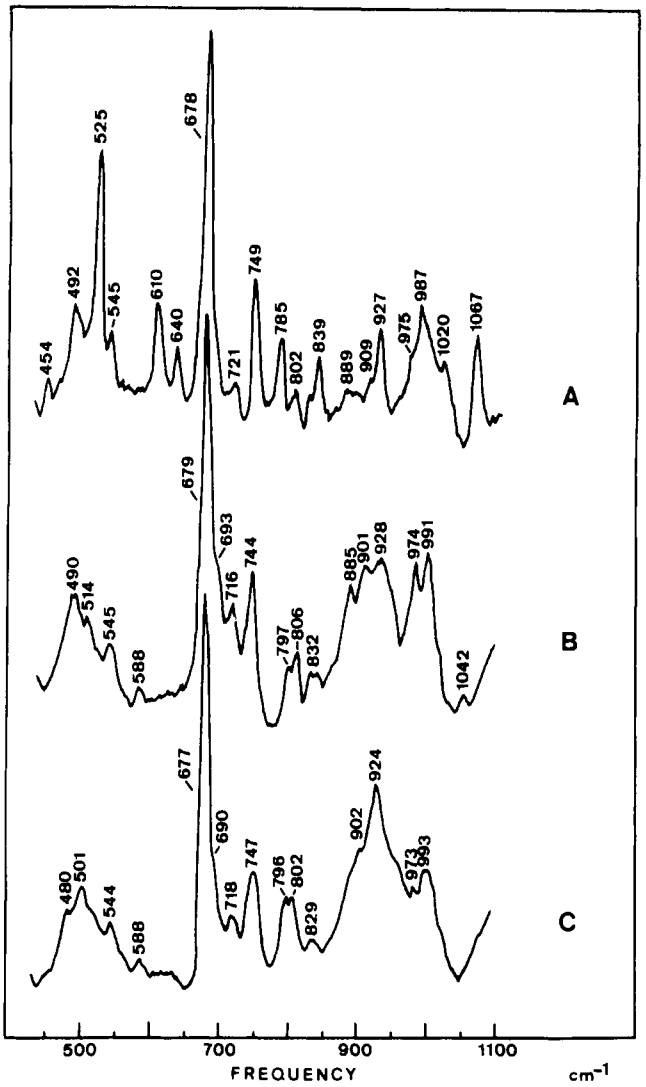

FIGURE 2: Medium-frequency regions (450–1050 cm^{-1}) of resonance Raman spectra of oxidized flavocytochrome b_2 (A), cytochrome b_2 core (B), and bis(imidazole) complex of ferriprotoporphyrin in 2% CTABr aqueous solution (C). Experimental conditions: see legend of Figure 1.

2A,B). These bands should arise from out of plane, pyrrole folding modes (Choi & Spiro, 1983), which are expected to be sensitive to heme–protein interactions (Kitagawa & Ozaki, 1987).

Lower Frequency Regions (150–450 cm^{-1}). The symmetric stretching mode of the iron to axial ligand bonds has been assigned to a band around 200 cm^{-1} in RR spectra of $Fe^{III}PP(ImH)_2$ (Desbois & Lutz, 1983; Mitchell et al., 1987). RR spectra of $Fe^{III}PP(ImH)_2$, cyt b_2(III), and flavocyt b_2(III) exhibit a band to band correspondence for the four bands observed in the 170–220-cm^{-1} region (Figure 3). On this basis, we propose that the 205-cm^{-1} band of cyt b_2(III) and flavocyt b_2(III) corresponds to the symmetric His–Fe(III)–His stretching mode.

Comparison of spectra A and B in Figure 3 indicates that low-frequency flavin modes are located at 425, 316, and 308 cm^{-1} in the spectra of flavocyt b_2(III).

The porphyrin modes ν_9 (269–271 cm^{-1}) and $2\nu_{35}$ (379–382 cm^{-1}) occur at essentially the same frequencies in RR spectra of $Fe^{III}PP(ImH)_2$ and of cyt b_2(III) and flavocyt b_2(III) (Figure 3). The ν_8 mode (346–350 cm^{-1}) occurs at a 3–4-cm^{-1} higher frequency in the latter two spectra than in that of $Fe^{III}PP(ImH)_2$. The 301- and 310-cm^{-1} bands of $Fe^{III}PP(ImH)_2$ may occur at 293 and 302 cm^{-1} for cyt b_2(III), respectively. Alternatively, the 310-cm^{-1} band of $Fe^{III}PP(ImH)_2$ may be correlated with the 293-cm^{-1} band of cyt b_2(III), without significant frequency change of the ~301-cm^{-1} band (Figure 3). The broad band at 422 cm^{-1} in the spectrum of $Fe^{III}PP(ImH)_2$ is apparently split into two components at 415 and 425 cm^{-1} in the spectrum of cyt b_2(III).

Reduced Forms of Flavocytochrome b_2, Cytochrome b_2 Core, and $FePP(ImH)_2$

Higher Frequency Regions (1000–1650 cm^{-1}). Comparisons of RR spectra of reduced forms of flavocyt b_2, cyt b_2 core, and

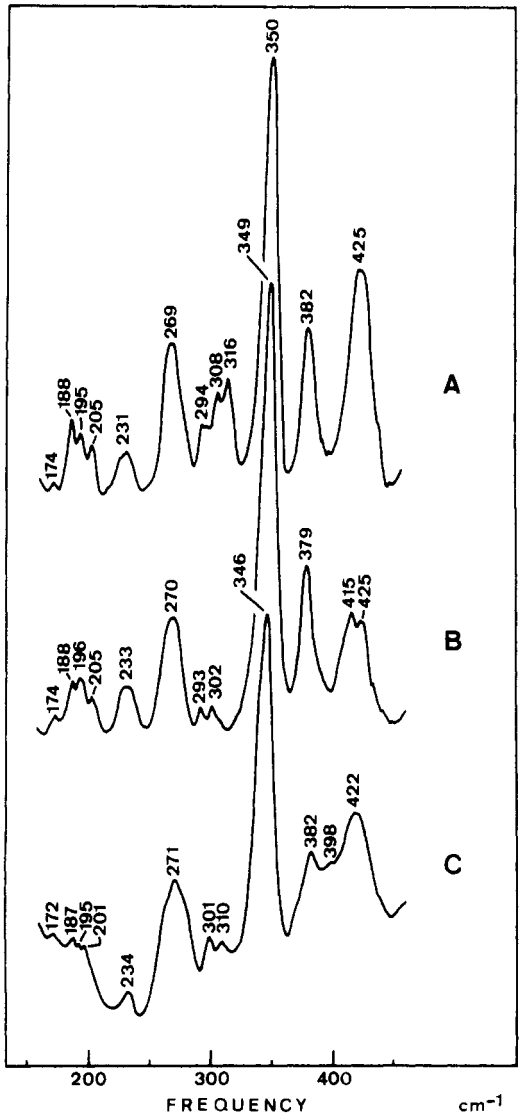

FIGURE 3: Low-frequency regions (150–450 cm^{-1}) of resonance Raman spectra of oxidized flavocytochrome b_2 (A), cytochrome b_2 core (B), and bis(imidazole) complex of ferriprotoporphyrin in 2% CTABr aqueous solution (C). Experimental conditions: see legend of Figure 1.

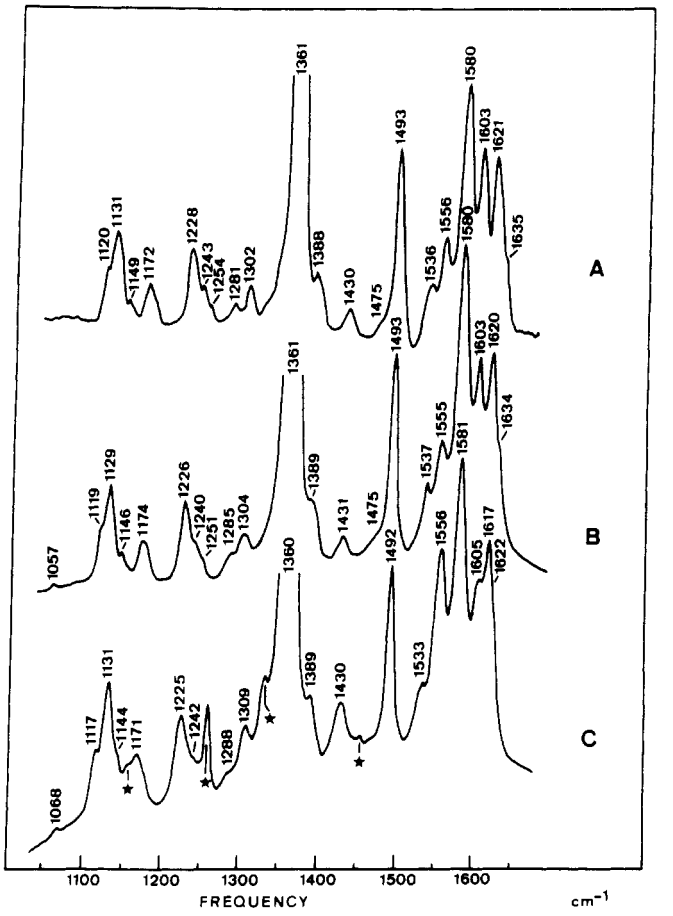

FIGURE 4: High-frequency regions (1050–1650 cm^{-1}) of resonance Raman spectra of reduced flavocytochrome b_2 (A), cytochrome b_2 core (B), and bis(imidazole) complex of ferroprotoporphyrin in 2% CTABr aqueous solution (C). Experimental conditions: see legend of Figure 1. The bands marked with a star below spectrum C are due to excess imidazole.

$FePP(ImH)_2$ excited at 441.6 nm clearly show that no sizable Raman band arises from the fully reduced flavins of flavocyt b_2(II) (Figure 4).

The core size markers ν_4, ν_3, ν_{38}, ν_{11}, ν_2, ν_{37}, and ν_{10} are observed at 1361, 1493, 1555, 1537, 1580, 1603, and 1620 cm^{-1}, in the spectra of cyt b_2(II) core, respectively (Figure 4). The frequencies of these modes do not exhibit any significant difference in the RR spectra of flavocyt b_2(II).

The $C_\alpha{=}C_\beta$ stretching mode of the vinyl groups of $Fe^{II}PP(ImH)_2$ has been previously assigned to the ca. 1620 cm^{-1} band largely overlapped by the ν_{10} mode at 1617 cm^{-1} (Choi et al., 1982a) (see also Figure 4C). The corresponding mode appears in RR spectra of flavocyt b_2(II) and of cyt b_2(II) as a shoulder at 1634–1635 cm^{-1} on the ν_{10} band (ca. 1620 cm^{-1}) (Figure 4A,B).

Medium-Frequency Regions (450–1000 cm^{-1}). Differences between RR spectra of $Fe^{II}PP(ImH)_2$, cyt b_2(II), and flavocyt b_2(II) essentially occur in the 450–500- and 900–1050-cm^{-1} ranges (Figure 5). In particular, the 922-cm^{-1} band of $Fe^{II}PP(ImH)_2$ is shifted up to ca. 927 cm^{-1} in the spectra of hemoproteins.

Lower Frequency Regions (150–450 cm^{-1}). By use of a $^{14}N_2(ImH) \rightarrow {}^{15}N_2(ImH)$ isotopic substitution, the symmetric stretching mode of the iron to axial ImH bonds was assigned to a 203-cm^{-1} RR band of $Fe^{II}PP(ImH)_2$ in an aqueous sodium dodecyl sulfate solution (Desbois & Lutz, 1981). This band is also observed at 203 cm^{-1} with CTABr as a detergent (Figure 6C). A comparison of the spectra of Figure 6 clearly shows that the 205-cm^{-1} band cannot arise from the flavin moiety. We then ascribe it to the His–Fe(II)–His symmetric stretching mode of flavocyt b_2 and cyt b_2(II).

Two deformation modes of the reduced porphyrin vinyl groups were characterized at ~410–425 cm^{-1} (Choi & Spiro, 1983). The RR spectra of Figure 6 show that the frequencies of these two modes are slighly higher for the hemoproteins than for $Fe^{II}PP(ImH)_2$.

Flavocytochrome b_2–Cytochrome c Interactions

Flavocytochrome b_2 is able to form reversible complexes with one or four molecules of yeast or mammalian cytochrome c per tetramer (Baudras et al., 1971; Prats, 1977). In order to detect possible structural changes induced on flavocyt b_2 by complexation with cyt c, we compared RR spectra of the free and complexed ferrous derivatives. For this purpose, mixtures of 1 equiv of cyt c(III)/tetramer of flavocyt b_2(III) were anaerobically reduced by L-lactate (10 equiv/tetramer) at pH 7.0 (10 mM phosphate buffer) in the Raman cell under vacuum. Electronic as well as RR spectra show that both flavocyt b_2 and cyt c are fully reduced and maintained in this stationary state in our experimental conditions. Since L-lactate is unable to directly reduce cyt c(III), this cyt c reduction obligatorily depends on the occurrence of a functional lactate–flavocyt

Table I: Frequencies (cm^{-1}) of Raman Bands of FMN Bound to Oxidized Flavocytochrome b_2 Compared to Averaged Frequencies for Flavin in Water from Published Raman Data on Riboflavin, FMN, and FAD in Water (Nishimura & Tsubol, 1978; Benecky et al., 1979; Dutta et al., 1980; Irwin et al., 1980; Schmidt et al., 1983; Copeland & Spiro, 1986)

flavocyt b_2	flavin moiety in water	frequency shift, $\delta(\Delta\nu)$[a]	band numbering[b]	assignment PED[c,d]	ring[d]	mode numbering[c]
1629	1631	−2	I	$\nu(C_8C_9)14$, $\nu(C_9C_{9a})14$	I	ν_6
1581	1584	−3	II	$\nu(N_1C_{10a})29$, $\nu(N_{10}C_{10a})19$	III, II	ν_8
1557	1550	+7	III	$\nu(N_1C_{10a})33$, $\nu(C_{4a}N_5)18$	III, II	ν_9
1501	1503	−2	IV	$\nu(C_{4a}N_5)33$, $\nu(C_{9a}N_{10})14$	II	ν_{10}
1463	1465	−2	V	$\nu(C_7C_8)20$, $\nu(C_8Me)15$	I	ν_{11}
1408	1412	−4	VI	$\nu(C_2N_3)33$, $\nu(C_2N_1)33$	III	ν_{14}
1360	1355	+5	VII	$\nu(C_{5a}C_6)17$, $\nu(N_{10}C_{10a})16$	I, II	ν_{15}
1302	1303	−1	VIII	$\nu(N_5C_{5a})30$, $\nu(C_8C_9)14$	II, I	ν_{16}
1284	1279	+5	IX	$\nu(C_{4a}C_{10a})22$, $\nu(C_4N_3)17$	III, II	ν_{17}
1257	1258	−1	X	$\nu(C_4N_3)43$, $\nu(C_4C_{4a})23$	III	ν_{18}
1231	1231	0	XI	$\nu(C_6C_7)17$, $\nu(C_8Me)16$	I	ν_{19}
1180	1185	−5	XII	$\nu(C_4H_{4a})13$, $\nu(C_{4a}C_{10a})12$	III, II	ν_{20}
1165	1163	+2	XIII	$\delta(C_6H)48$, $\nu(C_7Me)11$	I	ν_{21}
1131 1085	1144	−13		$\delta(C_9H)49$, $\delta(C_6H)15$	I	ν_{22}
1067	1069	−2	XIV	$\nu(C_2N_3)24$, $\nu(C_2N_1)23$	III	ν_{23}
839	835	+4		$\nu(C_9C_{9a})6$, $\delta(CN_5C)6$	I, II	ν_{26}
785	788	−3		$\nu(C_7Me)11$, $\delta(C_4{=}O)6$	I, III	ν_{27}
751	742	+9		$\nu(C_7C_8)24$, $\delta(CC_6C)9$	I	ν_{28}
640	633	+7		$\delta(CC_6C)9$, $\delta(CC_9C)9$	I	ν_{30}
610	605	+5		$\delta(CN_3C)_{20}$, $\delta(NC_{5a}C_6)6$	III, II, I	ν_{31}
525	522	+3		$\delta(C_8Me)$, $\delta(CC_7C)7$	I	ν_{33}
454	462	−8		$\delta(C_2{=}O)23$, $\delta(C_4{=}O)10$	III	ν_{35}
425	429	−4		$\delta(C_4{=}O)22$, $\delta(C_7Me)8$	III, I	ν_{36}
316 308	300	+16 +8		$\delta(N_{10}Me)11$, $\delta(C_8Me)9$	I	ν_{37}

[a] $\delta(\Delta\nu) = \Delta\nu$(flavoprotein) − $\Delta\nu$(flavin in water). [b] Band numbering according to Bowman and Spiro (1981). [c] Potential energy distribution (PED) and mode numbering according to Abe and Kyogoku (1987). [d] See Figure 9 for atom and ring numberings.

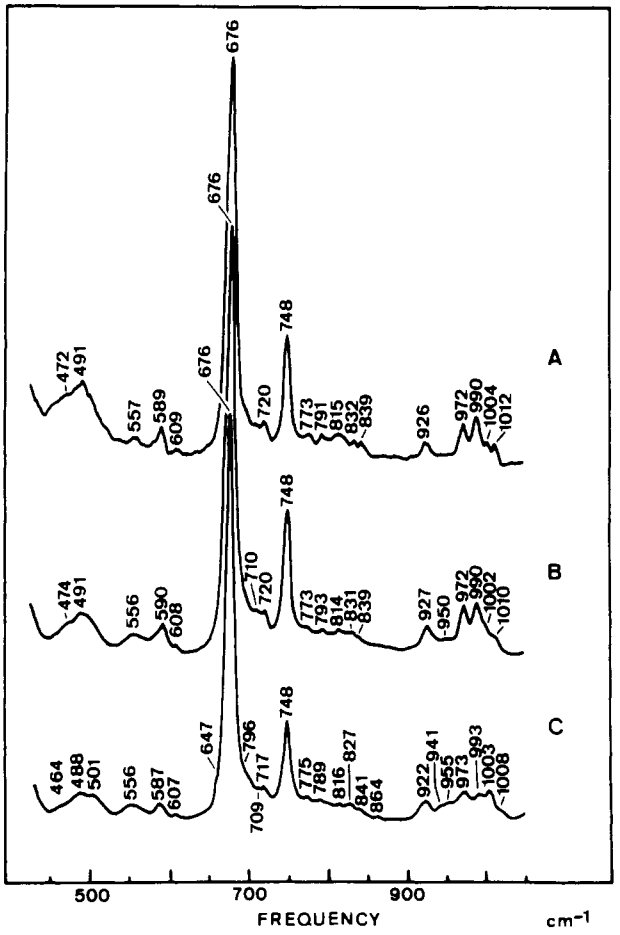

FIGURE 5: Medium-frequency regions (450–1050 cm^{-1}) of resonance Raman spectra of reduced flavocytochrome b_2 (A), cytochrome b_2 core (B), and bis(imidazole) complex of ferroprotoporphyrin in 2% CTABr aqueous solution (C). Experimental conditions: see legend of Figure 1.

b_2–cyt c complex (Capeillère-Blandin, 1982; Tegoni et al., 1983). Moreover, one may easily assume that the quantity of free cytochrome is negligible. Because marked differences distinguish RR spectra of b- and c-type hemes (Adar & Erecinska, 1978), RR spectra of this reduced flavocyt b_2–cyt c complex obtained with 441.6-nm excitation reveal a predominant contribution from flavocyt b_2(II). Unfortunately, no significant RR band shift can be associated with its complexation to cyt c(II). However, in order to evaluate relative intensity changes possibly induced in the RR bands of flavocyt b_2(II) and of cyt c(II) by their complexation, we computed differences between RR spectra of the complex and spectra of the isolated proteins. A more direct evaluation using internal, nonresonant, intensity standards was prevented by the fact that the complex is formed at low ionic strength only (Baudras et al., 1971). For example, Figure 7A presents the 650–800-cm^{-1} regions of RR spectra of flavocyt b_2–cyt c complex while spectra B and H of Figure 7 are of isolated flavocyt b_2(II) and cyt c(II), respectively. By subtraction of various contributions of spectrum B in spectrum A, the difference spectra C–G clearly show that the spectrum of bound cyt c(II) cannot be the same as that of isolated cyt c(II). Comparing spectrum E with spectrum H, we point out that the spectral changes between free and bound cyt c(II) concern strong intensity changes of the four main bands of this region (~679, 691, 701, and 753 cm^{-1}) without any significant change of their frequencies.

By use of similar spectral treatments, intensity modifications of several RR bands of cyt c(II) were also observed in the low-frequency regions (318, 329, 350, 359, 374, and 381 cm^{-1}) (spectra not shown).

In the high-frequency regions (1050–1700 cm^{-1}), these spectral computations clearly show that the intensities of some modes of both hemes b_2 and c are modified (Figure 8). The following bands of hemes b_2 are enhanced by complexation: 1149, 1303, 1555, and 1634 cm^{-1} (Figure 8A). The 1491- and

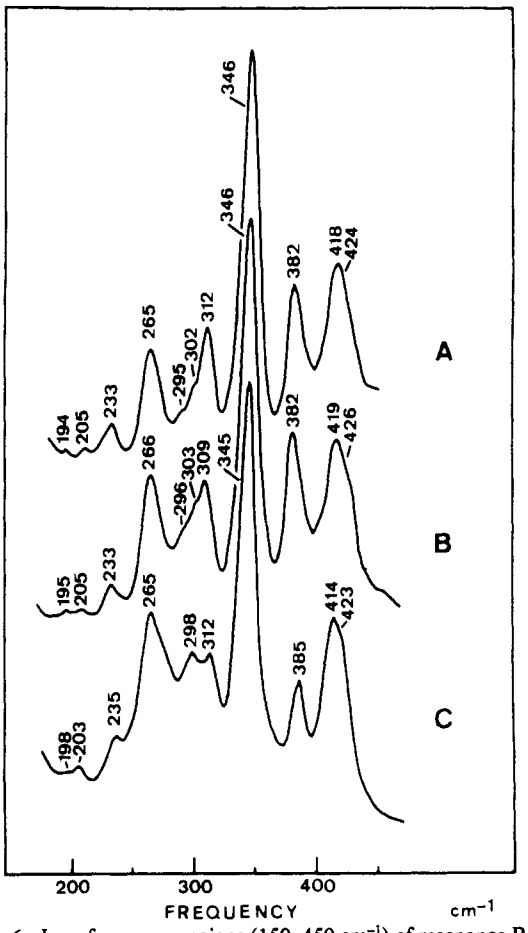

FIGURE 6: Low-frequency regions (150–450 cm^{-1}) of resonance Raman spectra of reduced flavocytochrome b_2 (A), cytochrome b_2 core (B), and bis(imidazole) complex of ferroprotoporphyrin in 2% CTABr aqueous solution (C). Experimental conditions: see legend of Figure 1.

1591-cm^{-1} bands of heme *c* are weakened in the complexation, while the 1087-, 1134-, 1169-, 1230-, 1392-, 1402-, and 1432-cm^{-1} bands are enhanced (Figure 8A).

In conclusion, although the precise stoichiometry of the flavocyt b_2–cyt *c* complex formed under our experimental conditions was not known, this RR study provides direct experimental evidence that the interactions between flavocyt b_2(II) and cyt *c*(II) can influence the heme modes. This phenomenon may reflect some discrete changes in the environments of both chromophores (hydrophobicity changes, polarity changes) without changes of their structures. The actual hypothesis of interactions between cyt *c*(II) and flavocyt b_2(II) localizes the regions of these interactions mainly at the level of the flavodehydrogenase domain (Thomas et al., 1983; Capeillère-Blandin & Albani, 1987). In fact, our experimental data could not directly evidence any possible interaction between heme *c* and flavodehydrogenase since the latter presents no RR signal with 441.6-nm excitation.

Discussion

Flavin Modes of Oxidized Flavocytochrome b_2

Raman Modes of Flavins and Structure of the Isoalloxazine Ring. RR spectra of flavocyt b_2(III) obtained at 441.6 nm contain 26 bands which we attribute to modes of bound FMN. Table I lists the frequencies of these bands in comparison to those previously obtained for the flavin moiety in water. Except for bands VIII, X, and XI, the observed FMN modes are significantly shifted by positive or negative values (Table I). These frequency changes [$\delta(\Delta\nu)$] reflect structural

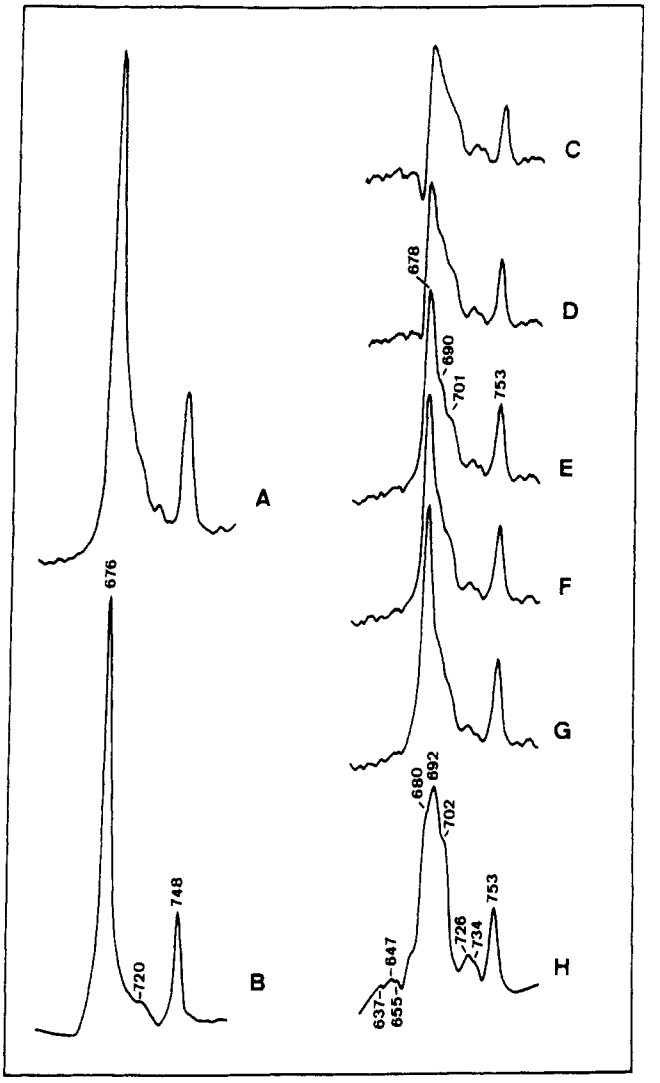

FIGURE 7: Portion of the medium-frequency regions (600–800 cm^{-1}) of resonance Raman spectra of reduced flavocytochrome b_2–cytochrome *c* complex (A), reduced isolated flavocytochrome b_2 (B), and reduced isolated horse cytochrome *c* (H). Spectra C–G are difference spectra: C = A − B; D = A − 0.9B; E = A − 0.8B; F = A − 0.7B; G = A − 0.6B. Experimental conditions: [flavocytochrome b_2] = 0.11 mM (tetramer); [lactate] = 1.1 mM; [cytochrome *c*] = 0.11 mM in 10 mM phosphate buffer, pH 7.0. See also legend of Figure 1.

alterations induced by the inclusion of the isoalloxazine ring in the protein. Unfortunately, the low resolution of X-ray data on flavocyt b_2 from *S. cerevisiae* (Xia et al., 1987; Mathews & Xia, 1987) prevents a very precise description of FMN–protein interactions.

However, the recent normal-mode calculations on lumiflavin by Abe and Kyogoku (1987) shed light on the assignments of the main RR bands of flavins. Indeed, although the nearly planar structure of the isoalloxazine macrocycle favors large coordinate mixing of in-plane skeleton modes, experimental data on model compounds have revealed a segregation of stretching modes localized in identifiable regions of the isoalloxazine ring (Nishina et al., 1978; Kitagawa et al., 1979; Müller et al., 1983; Abe et al., 1986). The vibrational analysis performed by Abe and Kyogoku (1987) closely reproduces the numbers, frequencies, and isotopic behaviors of high-frequency bands of lumiflavin (1000–1650 cm^{-1}). Therefore, it may reasonably by applied for any flavin-containing protein. These authors assigned almost pure ring I stretching vibrations to bands I (ν_6), V (ν_{11}), and XI (ν_{19}) (Table I, Figure 9). Skeletal stretching vibrations of ring III are found to be more or less

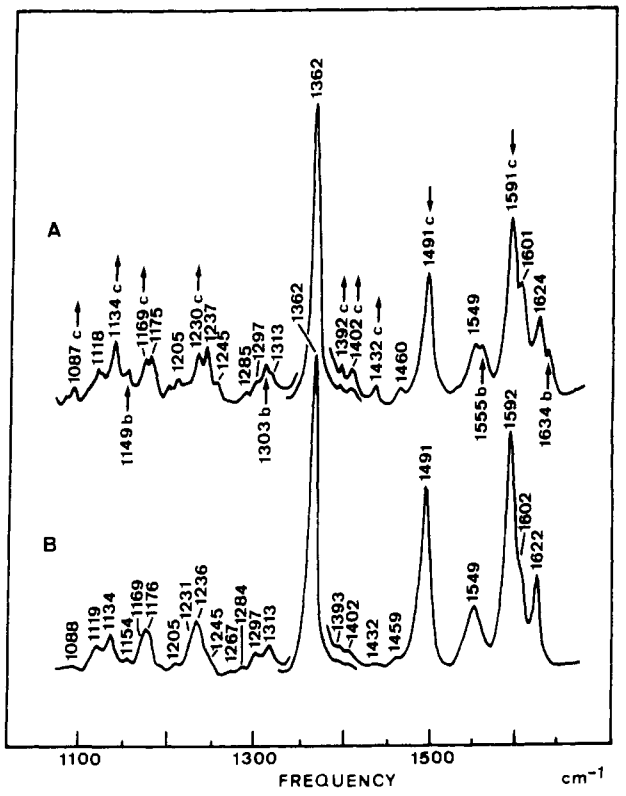

FIGURE 8: High-frequency regions (1050–1650 cm^{-1}) of computed difference RR spectra of reduced flavocytochrome b_2–cytochrome c complex minus isolated reduced flavocytochrome b_2 (A). For comparison, the spectra of isolated reduced horse cytochrome is shown in (B). The arrows under spectrum A indicate those RR bands of flavocytochrome b_2 which are enhanced in the spectra of the complex [see also Figure 4A for the spectrum of isolated flavocyt b_2(II)]. Arrows above spectrum A indicate those RR bands of cytochrome c(II) which are enhanced (↑) or weakened (↓) upon complexation with flavocytochrome b_2. Experimental conditions: see legends of Figures 1 and 7.

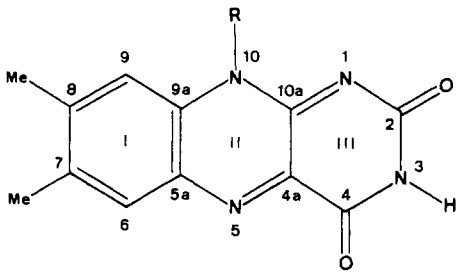

FIGURE 9: Structures of N^{10}-substituted isoalloxazines (Me = $-CH_3$): lumiflavin, R = $-CH_3$; riboflavin, R = $-CH_2(CHOH)_3CH_2OH$ (ribityl); flavin mononucleotide (FMN), R = ribityl phosphate; flavin adenine dinucleotide (FAD), R = ribityl diphosphate adenine.

coupled with a N(3)–H bending mode and have been assigned to bands VI (ν_{14}), IX (ν_{17}), X (ν_{18}), and XIV (ν_{23}). Finally, the symmetric and antisymmetric modes of N(5)–C(4a) and C(10a)–N(1) bonds have been assigned to bands II (ν_8) and III (ν_9), respectively (Abe & Kyogoku. 1987). These assignments make it possible to draw information about structural changes of the isoalloxazine macrocycle when it is included in a protein.

On the other hand, several flavoprotein structures are known from X-ray crystallographic studies. Among these, four flavoproteins have been investigated by both RR spectroscopy and X-ray crystallography, i.e., two flavodoxins, from *Desulfovibrio vulgaris* and *Clostridium* MP, a *p*-hydroxybenzoate hydrogenase, and a glutathione reductase (Watenpaugh et al., 1973; Burnett et al., 1974; Wierenga et al., 1979;

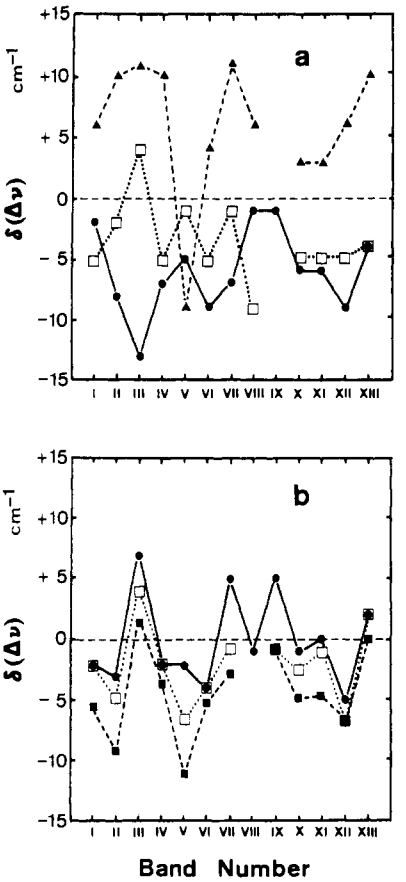

FIGURE 10: Diagrams of frequency shifts [$\delta(\Delta\nu)$] of high-frequency modes [bands I–XIII according to the numbering of Bowman and Spiro (1981)] of flavins induced by their binding to various flavoproteins. (a) Black triangles, lactate oxidase; open squares, luciferase–FMN complex; black circles, NADPH:cytochrome P-450 reductase. [The Raman data are from Visser et al., (1983) and Sugiyama et al. (1985).] (b) Black circles, flavocytochrome b_2(III); open squares, class B flavodoxins; black squares, class A flavodoxins. The diagram drawn for the class A flavodoxins is an average of Raman data on flavodoxins from *D. vulgaris*, *D. gigas*, *D. desulfuricans*, and *Azotobacter vinelandii* (Visser et al., 1983). The diagram drawn for the class B flavodoxins is an average of Raman data on flavodoxins from *Clostridium* MP, *C. kluyverii*, *C. formicoaceticum*, and *Megasphaera elsdenii* (Dutta & Spiro, 1980; Visser et al., 1983).

Hofsteenge et al., 1980; Dutta & Spiro, 1980; Bienstock et al., 1986; Schmith et al., 1983). Moreover, Raman data are available for other flavoproteins exhibiting various enzymatic activities (Morris & Bienstock, 1986; Mc Farland, 1987). Therefore, in order to handle all the shifts of high-frequency Raman bands for each flavoprotein, we propose the use of diagram plotting the frequency differences [$\delta(\Delta\nu)$] of Raman bands I–XIII (Table I) as a function of this band number (Figure 10). These representations are indeed expected to serve as structural standards, in an attempt to relate the topologies of the flavin proteic sites and/or their biological activities with the structure of the isoalloxazine nucleus of flavins.

Raman Diagrams and Biological Activities of Flavoproteins. The Raman diagrams of a series of flavoproteins endowed with different enzymatic activities (riboflavin binding protein, lactate oxidase, fatty acyl-coenzyme A dehydrogenase, glucose oxidase, glutathione reductase, *p*-hydroxybenzoate hydroxylase, NADPH:cytochrome P-450 reductase, luciferase–FMN complex, and flavodoxins) have been drawn from available Raman data (Kitagawa et al., 1979; Benecky et al., 1979; Visser et al., 1983; Schmidt et al., 1983; Sugiyama et al., 1985; Bienstock et al., 1986) (Figure 10 and figure not shown). Most of these diagrams strongly differ from each

other (Figure 10a), indicating that expectedly different biological activities are associated with different flavin structures. However, the Raman diagrams of flavodoxins and flavocytochrome b_2 present obvious homologies (Figure 10b).

Flavodoxins are pure electron transferases (Hemmerich & Massey, 1982) which can be divided into two types depending on their spectral and biological properties (D'Anna & Tollin, 1972), i.e., the so-called *rubrum* type (class A flavodoxins), such as *D. vulgaris* flavodoxin, and the *pasteurianum* type (class B flavodoxins), such as *Clostridium* MP flavodoxin. The X-ray structures of the FMN sites of the two types also exhibit strong differences, i.e., in the number and location of H-bonds at rings II and III and in the aromatic environments of ring I (Watenpaugh et al., 1973; Burnett et al., 1974). Flavocyt b_2 has a dehydrogenase/electron transferase activity. Its three-dimensional structure (Xia et al., 1987; Mathews & Xia, 1987) indicates that the four flavin sites differ completely from those of flavodoxins. These observations have two consequences: (i) the structure of the FMN macrocycle cannot be deduced by simple site comparisons, and (ii) different FMN–protein interactions can have similar effects on the structure and electron distribution at the isoalloxazine nucleus. The homologies observed between the Raman diagrams of these proteins are thus remarkable. They indicate closely similar electron distributions at the macrocycle, despite the very different isoalloxazine–protein interactions occurring between class A flavodoxins, class B flavodoxins, and flavocytochrome b_2 (Watenpaugh et al., 1973; Burnett et al., 1974; Xia et al., 1987; Mathews & Xia, 1987; Lederer & Mathews, 1987).

One may note, also, that the Raman diagram of the luciferase–FMN complex (Visser et al., 1983) presents some analogy, in the band II to band VII region, with those of flavodoxins (Figure 10). This analogy however is not very close, in agreement with recent NMR data (Vervoort et al., 1985, 1986). On the other hand, the Raman diagram of NADPH:cytochrome P-450 reductase presents close analogies with that of flavocyt b_2 in the region of bands IV–XIII. We may add that these two proteins have a dehydrogenase/electron transferase activity (Hemmerich & Massey, 1982). Therefore, the fingerprints presented in Figure 10 appear to a large extent related to the biological activity of flavoproteins.

The Raman diagrams show that the frequency shifts observed for any given protein are essentially positive or essentially negative (Figure 10 and figure not shown). Since the isoalloxazine ring is highly conjugated, one may assume that a significant electronic perturbation at a particular atom is expected to be in great part transmitted in the entire π-system. Therefore, the direction of shifts of $\delta(\Delta\nu)$ is expected to be related to the electron density at the macrocycle, a positive shift corresponding to an increased electron density (Visser et al., 1983). Comparing the diagram of flavocyt b_2 with that of class A or class B flavodoxins (Figure 10b) indicates that the electron density at the isoalloxazine ring is higher for flavocyt b_2. This parameter may play a major role in the formation and possibly the stabilization of the type of semiquinone, red anionic for flavocyt b_2 and blue neutral for the flavodoxins.

Environment of the Isoalloxazine Ring of FMN in Flavocyt b_2. A careful inspection of X-ray data available for the flavoproteins indicates that four factors can influence the electron distribution and the electron density at the isoalloxazine ring: (i) the number and strength of H-bonds at ring III; (ii) the presence of an H-bond at the N(5) atom of ring II; (iii) the interactions of aromatic amino acid side chains with ring I; (iv) the solvent accessibility and the polar character of the isoalloxazine site (Watenpaugh et al., 1982; Burnett et al., 1974; Wierenga et al., 1979; Hofsteenge et al., 1980; Schulz et al., 1982; Karplus & Schulz, 1987). The higher electron density at the isoalloxazine macrocycle of flavocyt b_2 than at those of flavodoxins, as indicated by the Raman diagrams, thus may originate from an increased H-bonding at ring III. Indeed, stretching modes essentially involving ring III (ν_8, ν_9, ν_{14}, ν_{17}, ν_{18}, and ν_{23}) are the most affected by the FMN–protein interactions since $\delta(\Delta\nu)$ varies between −4 and +7 cm^{-1} (Table I). These shifts are indicative of strong H-bondings at ring III considering both Raman and X-ray data on flavodoxins (Visser et al., 1983; Dutta & Spiro, 1980; Watenpaugh et al., 1972; Burnett et al., 1974). The crystallographic data on flavocyt b_2 from *S. cerevisiae* tend to confirm this suggestion since four potential hydrogen-bond donors or acceptors are present around the four possible H-bonding positions of the pyrimidine ring (Ser-228, Glu-252, Thr-280, and Lys-349) (Lederer & Mathews, 1987). On the other hand, the stretching modes in which the N(5) atom of ring II is strongly involved are ν_{10} and ν_{16}. They exhibit weak frequency differences (−1 and −2 cm^{-1}) when FMN is in water or included in flavocyt b_2 (Table I). Therefore, the N(5) atom of FMN exhibits similar hydrogen bonding in water and in flavocyt b_2. This isoalloxazine site, which has a good electron-acceptor capacity (Platenkamp et al., 1987) is the likely site for electron transfer between lactate and FMN (Lederer & Mathews, 1987). Finally, stretching modes essentially involving ring I (ν_6, ν_{11}, and ν_{19}) are also weakly affected ($-2\ cm^{-1} \leq \delta(\Delta\nu) \leq 0\ cm^{-1}$) by the FMN–protein interaction in flavocyt b_2(III) (Table I). Although FMN stacking hardly affects its Raman spectrum (Schmidt et al., 1983), these small differences may occur from those stacking interactions of FMN with Tyr-143 and -144 suggested to occur in flavocyt b_2 by recent X-ray data (Lederer & Mathews, 1987).

Porphyrin Skeletal Modes of Hemes b_2

Table II lists the frequencies of core size marker bands which are Raman active with 441.6-nm excitation of oxidized or reduced flavocyt b_2, cyt b_2, and $FePP(ImH)_2$ (ν_{10}, ν_{37}, ν_2, ν_{38}, ν_{11}, ν_3, and ν_4). Using the relation $d = A - \nu/K$, where A and K are constants depending on the mode number (Parthasarathi et al., 1987), we have calculated the distance d (in Å) between the porphyrin center and the N(pyrrole) atoms from the mode frequency ν (in cm^{-1}). Calculations on the ν_{10}, ν_{37}, ν_2, ν_{11}, ν_{38}, ν_3, and ν_4 modes give an averaged distance d of 2.022 Å for both flavocyt b_2(II) and cyt b_2(II). Distance d is similarly calculated to be 1.990 Å for the oxidized forms of both hemoproteins with the frequency of the ν_{10}, ν_{37}, ν_2, ν_{38}, ν_3, and ν_4 modes (Table II). These data clearly show that the heme globules of the flavoenzyme impose the heme structures without detectable influence from the flavin domains as already suggested from spectroscopic data (visible absorption, EPR, and NMR) (Labeyrie et al., 1966; Watari et al., 1967; Pajot & Groudinsky, 1970; Labeyrie et al., 1988) as well as from potentiometric redox titrations (Silvestrini et al., 1986).

In the lower frequency regions, the RR band assigned to mode ν_9 is observed at 269–270 cm^{-1} for the oxidized states of flavocyt b_2 and cyt b_2 and at 265–266 cm^{-1} for the reduced forms. These frequencies are both characteristic of iron–protoporphyrin complexes with the metal atom in the porphyrin plane (Desbois & Lutz, 1981, 1983). Therefore, the iron–N(pyrrole) bond lengths must be equal to the porphyrin center–N(pyrrole) distances calculated above, in both the oxidized and reduced states. The Fe–N(pyrrole) bond lengths of low-spin ferro- and ferriheme complexes fall in the 1.997

Table II: Frequencies (cm^{-1}) of Porphyrin Skeletal Modes of Oxidized and Reduced Flavocyt b_2, Cyt b_2 Core, and $FePP(ImH)_2$

mode[a]	flavocyt b_2(III)	cyt b_2(III)	$Fe^{III}PP(ImH)_2$	flavocyt b_2(II)	cyt b_2(II	$Fe^{II}PP(ImH)_2$	assignment[b]
ν_{10}	1640	1640	1638	1620	1620	1617	$\nu(C_aC_m)$
ν_{37}	1598	1597	1596	1603	1603	1605	$\nu(C_bC_b)$
ν_2	1579	1579	1579	1580	1580	1581	$\nu(C_bC_b)$
ν_{38}	1557	1557	1554	1556	1555	1556	$\nu(C_bC_b)$
ν_{11}				1536	1537	1533	$\nu(C_bC_b)$
ν_3	1505	1505	1504	1493	1493	1492	$\nu(C_aC_m)$
ν_{28}		1469	1475	1475	1475		$\nu(C_aC_m)$
ν_{20}		1395		1388	1389	1389	$\nu(C_aN)$
ν_4	1374	1374	1374	1361	1361	1360	$\nu(C_aN)$
		1153		1149	1146	1144	
$\nu_6 + \nu_8$		1127	1132	1131	1129	1131	
ν_{22}			1127				$\nu(C_aN)$
ν_{45}		991	993	990	990	993	$\nu(C_aN)$
$\nu_{32} + \nu_{35}$	975	974	973	972	972	973	
ν_6	802	806	802	815	814	816	$\delta(C_aC_mC_a)$
ν_{16}		744	747	748	748	748	$\delta(C_aNC_a)$
ν_7	678	679	677	676	676	675	$\delta(C_bC_aN)$
ν_{49}	545	545	544	557	556	556	$\delta(C_aC_bC_b)$
		514	501	491	491	501	pyr fold
	492	490	488	472	474	488	pyr fold
$2\nu_{35}$	382	379	382	382	382	385	
		302	301	295	296	298	$\gamma(C_mC_a)$
ν_9	269	270	271	265	266	265	pyr tilt + ν(Fe–N)
	231	233	234	233	233	235	

[a] Mode numbering according to Abe et al. (1978) and Kitagawa et al. (1978). [b] Assignment according to Abe et al. (1978), Choi et al. (1982a,b), and Desbois et al. (1984).

Table III: Frequencies (cm^{-1}) of Peripheral Heme Modes of Oxidized and Reduced Flavocyt b_2, Cyt b_2 Core, and $FePP(ImH)_2$

mode[a]	flavocyt b_2(III)	cyt b_2(III)	$Fe^{III}PP(ImH)_2$	flavocyt b_2(II)	cyt b_2(II)	$Fe^{II}PP(ImH)_2$	assignment[b]
	1636	1634	1620	1635	1634	1620	$\nu(C_\alpha C_\beta$vinyl)
	1429	1431	1433	1430	1431	1430	$\delta_S(=CH_2$vinyl)
	1329	1332	1344				$\delta(C_m–H)$ +
ν_{21}	1307	1308	1308	1302	1304	1309	δ(—C=vinyl)
ν_{13}		1232	1232	1228	1226	1225	$\delta(C_m–H)$
		1172	1169	1172	1174	1171	$\delta(C_b–C_\alpha$vinyl)
	1085	1088	1093				
				1012	1010	1008	γ(CH=vinyl)
ν_{46}		928	924	926	927	922	$\nu(C_b–S)$
				839	839	841	$\gamma(C_m–H)$
ν_{32}		797	796	791	793	789	$\delta(C_b–S)$
ν_{47}	721	716	718	720	720	717	$\delta(C_b–S)$
		588	588	589	590	587	$\delta(C_b–S)$
		425	422	424	426	423	$\delta(C_bC_\alpha C_\beta$vinyl)
		415		418	419	414	
ν_8	350	349	346	346	346	345	$\delta(C_b–S)$
ν_{50} or	294	293	310	311	309	312	$\delta(C_b–S)$
ν_{51}				302	303		

[a] Mode numbering according to Abe et al. (1978). [b] Assignment according to Choi et al. (1982a,b), Desbois et al. (1984), and Lee et al. (1986).

(±0.014) and 1.986 (±0.010) Å ranges, respectively (Scheidt & Gouterman, 1983). Oxidation of the iron atom thus induces a 0.011 (±0.024 Å) shortening of these bonds. The present calculations indicate that the corresponding change in cyt b_2 and flavocyt b_2 is −0.032 Å. This value is thus one of the largest oxidation-induced shortening observed for the Fe–N(pyrrole) length in hemes.

Inspection of Table II indicates that the stretching frequencies of the porphyrin macrocycle do not differ significantly among flavocyt b_2, cyt b_2, and $FePP(ImH)_2$ in a given oxidation state. However, some deformation modes occur at different frequencies in the hemoproteins and in the model compounds (Table II). Among these, the folding modes of the pyrrole rings (480–515 cm^{-1}) appear to be particularly sensitive to protein–porphyrin interactions.

Modes Involving the Peripheral Groups of Protoheme

Systematic studies have shown that some modes of peripheral groups of heme are active in RR spectra of metalloporphyrin derivatives (Tsubaki et al., 1980; Desbois et al., 1984). More precisely, selective deuterations at the peripheral substituents as well as normal coordinate treatments have identified vinyl and methyl vibrations in RR spectra of protoheme (Choi et al., 1982a,b; Lee et al., 1986). Following these assignments, the C_α=C_β (vinyl) stretching mode occurs at ~1635 cm^{-1} in both flavocyt b_2 and cyt b_2, i.e., at a frequency ca. 15 cm^{-1} higher than those of the model compounds $Fe^{II}PP(ImH)_2$ and $Fe^{III}PP(ImH)_2$ (Table III). As for these models, the frequency of this mode is insensitive to the oxidation state of the iron atom. The frequencies of the C_b–C_α (vinyl) stretching mode at ~1173 cm^{-1} and of the two components of the C_b—C_α=C_β (vinyl) deformation at ~425 and 418 cm^{-1} are also upshifted in cyt b_2 and flavocyt b_2 relative to those of the model compounds, although less than the stretching mode (Table III). These three upshifted frequencies show that the electron densities at the three C_b (pyrrole), C_α and C_β (vinyl) atoms must be higher in cyt b_2 or flavocyt b_2 than in $FePP(ImH)_2$. This indicates increased electron-withdrawing capabilities of these groupings, likely due to their increased conjugations with the porphyrin macrocycle and itself

likely originating from changes in the vinyl conformations. In $Fe^{III}PP(1MeIm)_2$, the 2- and 4-vinyl groups are not coplanar with their respective pyrrole rings with which they make 24° and 41° dihedral angles, respectively (Little et al., 1975). A compilation of crystallographic data show that, in hemoproteins, the 2-vinyl group varies from being coplanar with pyrrole ring I to being 59° out-of-plane, while the 4-vinyl group ranges from being coplanar to being roughly orthogonal to pyrrole ring II (Reid et al., 1986).

X-ray data on oxidized cyt b_5 show that the vinyl groups are nearly in the pyrrole planes (Mathews, 1980; Reid et al., 1986). Unfortunately, the frequencies of RR vinyl modes of this hemoprotein are not known. Nevertheless, the heme binding fragment of cyt b_5 exhibits a sequence homology with that of the b_2 core, except for a 12-residue segment starting after His-59 of the b_2 core (Guiard et al., 1974; Haumont et al., 1987). Taken together, these data therefore strongly suggest that, as for cyt b_5, amino acids of the heme b_2 pocket impose a coplanarity of vinyl groups with their respective pyrrole rings, thus increasing their electron-withdrawing capabilities.

Axial Ligation of Cyt b_2 and Flavocyt b_2

The heme axial ligands, namely, histidyl imidazole side chains (Groudinsky, 1971), are expected to be His-36 and His-59 (Guiard et al., 1974; Haumont et al., 1987). The recent crystallographic data on flavocyt b_2 support this prediction (Xia et al., 1987). The symmetric stretching mode of the bonds between the axial imidazoles and the iron atom has been assigned to a band at 200–203 cm^{-1} in RR spectra of $Fe^{II}PP(ImH)_2$ and $Fe^{III}PP(ImH)_2$ (Desbois & Lutz, 1981, 1983; Mitchell et al., 1987). We assign the 203- and 201-cm^{-1} bands present in RR spectra of $Fe^{II}PP(ImH)_2$ and $Fe^{III}PP(ImH)_2$ in aqueous CTABr solutions to the same mode, respectively. Indeed, perdeuteration of the axial ligands ($[H_4]ImH \rightarrow [^2H_4]ImH$) induces 4- and 5-$cm^{-1}$ downshifts of these two bands, respectively (Desbois and Lutz, unpublished data). The band to band correspondence observed in the 170–280-cm^{-1} regions of RR spectra of cyt b_2, flavocyt b_2, and model compounds (Figures 3 and 6) strongly supports the assignment of the 205-cm^{-1} band of oxidized or reduced b_2 core and flavocyt b_2 to the symmetric His–Fe–His stretching mode. This 205-cm^{-1} wavenumber indicates rather strong Fe–His bonds in cyt b_2 and flavocyt b_2. Indeed, the symmetric stretching mode of 1-methylimidazole (1MeIm) ligands with the iron atom of $Fe^{II}PP(1MeIm)_2$ was proposed to be at 194 cm^{-1} (Desbois & Lutz, 1981, 1983). This assignment was recently supported by the observation of an 8-cm^{-1} downshift of the 194-cm^{-1} band of $Fe^{II}PP(1MeIm)_2$ in water upon perdeuteration of the axial ligands ($[H_6]$-1MeIm $\rightarrow$ $[^2H_6]$-1MeIM) (Desbois and Lutz, unpublished data). The change (Δr) in the Fe–N (axial ligand) bond length in passing from $Fe^{II}PP(1MeIm)_2$ to ferrous cyt b_2 or flavocyt b_2 can be estimated from the frequencies of their ν(ligand–Fe–ligand) modes, by use of the Herschbach and Laurie (1961) rule:

$$\Delta r = 1.2 \log (\nu/\nu')$$

This relation is valid under the assumption that the axial ligands 1MeIm and His have the same effective mass (which is not necessarily 82 amu) [cf. Desbois and Lutz (1983) and Mitchell et al. (1987)]. Taking ν = 205 cm^{-1} and ν' = 194 cm^{-1}, Δr is 0.029 Å. X-ray crystallographic data on $Fe^{II}TPP(1MeIm)_2$ give a Fe–N(1MeIm) bond length of 2.014 (5) Å (Scheidt & Gouterman, 1983). Assuming that this distance is porphyrin independent (Hoard, 1975; Scheidt & Gouterman, 1983), the Fe–N(His) distance in cyt b_2 and flavocyt b_2 is so estimated to be 1.985 (5) Å, a plausible value (Takano & Dickerson, 1980).

The identical, 205-cm^{-1} value observed for the ν(His–Fe–His) mode of both cyt b_2 and flavocyt b_2, in both their oxidized and reduced states, indicates that the axial bond lengths are independent from the iron oxidation state and are not perturbed by the interactions between the cyt b_2 and flavin domains in the enzyme.

As cyt b_2(II), cyt b_5(II) is unable to bind carbon monoxide (Mathews, 1985). On the contrary, the reduced cytochromes c_3 react with this gaseous ligand (Meyer & Kamen, 1982). Yet, these three hemoproteins most probably share high-frequency values of the His–Fe(II)–His stretching mode. Indeed, a 206-cm^{-1} RR band has been ascribed to this mode in the spectra of cyt c_3(II) from *D. vulgaris* (Desbois & Lutz, 1984). RR spectra of reduced, native cyt b_5(II) contain a weak 209-cm^{-1} band (Kitagawa et al., 1982), which constitutes a good candidate for the ν(His–Fe–His) mode. As a consequence, since the Fe(II)–His bond strengths of these three hemoproteins are practically the same, the CO molecule is likely able to displace one of these bonds in cyt b_2(II) and cyt b_5(II). Therefore, the different behaviors to CO ligation appear to correspond to a difference in heme accessibility.

Conclusions

This RR investigation on isolated flavocyt b_2 and cyt b_2 "core" helps characterize the heme structure in its oxidized and reduced state and the flavin structure and environment in oxidized flavocyt b_2. These data show the absence of an influence of the flavin domains on the heme structures in the enzyme. The axial and peripheral interactions between heme b_2 and the cytochrome pocket are strong and not modified by a change in oxidation state of the iron atom. Moreover, the present Raman investigation on the flavocyt b_2(II)–cyt c(II) complex has revealed that the protein interactions can influence the intensities of several porphyrin modes of both heme types. Finally, a comparison of various flavoenzymes allowed us to propose relationships between their biological activities and the Raman shifts of high-frequency flavin modes.

Acknowledgments

We thank Drs. R. Cassoly and Y. Henry for their helpful comments on the manuscript, L. Naslin and A. Lebozec for the preparation of *H. anomala* flavocytochrome b_2, and M. Duponchelle for the realization of this paper.

References

Abe, M., & Kyogoku, Y. (1987) *Spectrochim. Acta 43A*, 1027–1037.

Abe, M., Kitagawa, T., & Kyogoku, Y. (1978) *J. Chem. Phys. 69*, 4526–4534.

Abe, M., Kyogoku, Y., Kitagawa, T., Kawano, K., Ohishi, N., Takai-Susuki, A., & Yagi, K. (1986) *Spectrochim. Acta 42A*, 1059–1068.

Adar, F., & Erecinska, M. (1978) *Biochemistry 17*, 5484–5488.

Appleby, C. A., & Morton, R. K. (1959) *Biochem. J. 71*, 492–499.

Baudras, A., Krupa, M., & Labeyrie, F. (1971) *Eur. J. Biochem. 20*, 58–64.

Benecky, M., Li, T. Y., Schmidt, J., Frerman, F., Watters, K. L., & Mc Farland, J. (1979) *Biochemistry 18*, 3471–3476.

Bienstock, R. J., Schopfer, L. M., & Morris, M. D. (1986) *J. Am. Chem. Soc. 108*, 1833–1838.

Bowman, W. D., & Spiro, T. G. (1981) *Biochemistry 20*, 3313–3318.
Burnett, R. M., Darling, G. D., Kendall, D. S., LeQuesne, M. E., Mayhew, S. G., Smith, W. W., & Ludwig, M. L. (1974) *J. Biol. Chem. 249*, 4383–4392.
Capeillère-Blandin, C. (1982) *Eur. J. Biochem. 128*, 533–542.
Capeillère-Blandin, C., & Albani, J. (1987) *Biochem. J. 245*, 159–165.
Celerier, J., Risler, Y. Schwenke, J., Janot, J. M., & Gervais, M. (1989) *Eur. J. Biochem.* (in press).
Choi, S., & Spiro, T. G (1983) *J. Am. Chem. Soc. 105*, 3683–3692.
Choi, S., Spiro, T. G., Langry, K. C., & Smith, K. M. (1982a) *J. Am. Chem. Soc. 104*, 4337–4344.
Choi, S., Spiro, T. G., Langry, K. C., Smith, K. M., Bredd, D. L., & La Mar, G. N. (1982b) *J. Am. Chem. Soc. 104*, 4345–4351.
Copeland, R. A., & Spiro, T. G. (1986) *J. Phys. Chem. 90*, 6648–6654.
D'Anna, J. A., & Tollin, G. (1972) *Biochemistry 11*, 1073–1080.
Desbois, A., & Lutz, M. (1981) *Biochim. Biophys. Acta 671*, 168–176.
Desbois, A., & Lutz, M. (1983) in *Hemoglobin* (Schnek, A. G., & Paul, C., Eds.) pp 285–297, University of Brussels, Brussels.
Desbois, A., & Lutz, M. (1984) *Proceedings of the IXth International Conference on Raman Spectroscopy*, pp 480–481, The Chemical Society of Japan, Tokyo, Japan.
Desbois, A., Lutz, M., & Banerjee, R. (1979) *Biochemistry 18*, 1510–1518.
Desbois, A., Henry, Y., & Lutz, M. (1984) *Biochim. Biophys. Acta 785*, 148–160.
Desbois, A., Tegoni, M., Gervais, M., & Lutz, M. (1988) *Proceedings of the XIth International Conference on Raman Spectroscopy* (Clark, R. J. H., & Long, D. A., Eds.) pp 677–678, Wiley, Chichester, U.K.
Dutta, P. K., & Spiro, T. G. (1980) *Biochemistry 19*, 1590–1593.
Gervais, M., Groudinsky, O., Risler, Y., & Labeyrie, F. (1977) *Biochem. Biophys. Res. Commun. 77*, 1543–1551.
Gervais, M., Labeyrie, F., Risler, Y., & Vergnes, O. (1980) *Eur. J. Biochem. 111*, 17–31.
Gervais, M., Risler, Y., & Corazzin, S. (1983) *Eur. J. Biochem. 130*, 253–259.
Groudinsky, O. (1971) *Eur. J. Biochem. 18*, 480–484.
Guiard, B., Groudinsky, O., & Lederer, F. (1974) *Proc. Natl. Acad. Sci. U.S.A. 71*, 2539–2543.
Haumont, P.-Y., Thomas, M.-A., Labeyrie, F., & Lederer, F. (1987) *Eur. J. Biochem. 169*, 539–546.
Hemmerich, P., & Massey, V. (1982) in *Oxidases and Related Redox Systems* (King, T. E., Mason, H. S., & Morrison, M., Eds.) pp 379–405, Pergamon Press, Oxford.
Herschbach, D. R., & Laurie, V. W. (1961) *J. Chem. Phys. 35*, 458–463.
Hoard, J. L. (1975) in *Porphyrins and Metalloporphyrins* (Smith, K. M., Eds.) pp 317–380, Elsevier, Amsterdam.
Hofsteenge, J., Vereijken, J. M., Weijer, W. J., Beintema, J. J., Weirenga, R. K., & Drenth, J. (1980) *Eur. J. Biochem. 113*, 141–150.
Irwin, R. M., Visser, A. J. W. G., Lee, J., & Carreira, L. A. (1980) *Biochemistry 19*, 4639–4646.
Karplus, P. A., & Schulz, G. E. (1987) *J. Mol. Biol. 195*, 701–729.
Kitagawa, T., & Nagai, K. (1979) *Nature 281*, 503–504.
Kitagawa, T., & Ozaki, Y. (1987) *Structure Bonding 64*, 71–114.
Kitagawa, T., Abe, M., & Ogoshi, H. (1978) *J. Chem. Phys. 69*, 4516–4525.
Kitagawa, T., Nishina, Y., Kyogoku, Y., Yamano, T., Ohishi, N., Suzuki, A. T., & Yagi, K. (1979) *Biochemistry 18*, 1804–1808.
Kitagawa, T., Fukumori, Y., & Yamanaka, T. (1980) *Biochemistry 19*, 5721–5729.
Kitagawa, T., Sugiyama, T., & Yamano, T. (1982) *Biochemistry 21*, 1680–1686.
Labeyrie, F. (1982) in *Flavins and Flavoproteins* (Massey, V., & Williams, C. H., Eds.) pp 823–832, Elsevier, Amsterdam.
Labeyrie, F., Groudinsky, O., Jacquot-Armand, Y., & Naslin, L. (1966) *Biochim. Biophys. Acta 128*, 492–503.
Labeyrie, F., Baudras, A., & Lederer, F. (1978) *Methods Enzymol. 53*, 238–256.
Labeyrie, F., Beloeil, J.-C., & Thomas, M.-A. (1988) *Biochim. Biophys. Acta 953*, 134–141.
Lederer, F., & Mathews, F. S. (1977) in *Flavins and Flavoproteins* (Mc Cormick, D. B., & Edmonson, D. E., Eds.) pp 133–142, Walter de Gruyter, Berlin.
Lee, H., Kitagawa, T., Abe, M., Pandey, R. K., Leung, H.-K., & Smith, K. M. (1986) *J. Mol. Struct. 146*, 329–347.
Little, R. G., Dymock, K. R., & Ibers, J. A. (1975) *J. Am. Chem. Soc. 97*, 4532–4539.
Mathews, F. S. (1980) *Biochim. Biophys. Acta 622*, 375–379.
Mathews, F. S. (1985) *Prog. Biophys. Mol. Biol. 45*, 1–56.
Mathews, F. S., & Xia, Z.-X. (1987) in *Flavins and Flavoproteins* (Mc Cormick, D. B., & Edmonson, D. E., Eds.) pp 123–132, Walter de Gruyter, Berlin.
Mc Farland, J. T. (1987) in *Biological Applications of Raman Spectroscopy*. Vol. 2, Resonance Raman Spectra of Polyenes and Aromatics (Spiro, T. G., Ed.) pp 211–302, Wiley, New York.
Meyer, T. E., & Kamen, M. D. (1982) *Adv. Protein Chem. 35*, 105–212.
Mitchell, M. L., Li, X.-Y., Kincaid, J. R., & Spiro, T. G. (1987) *J. Phys. Chem. 91*, 4690–4696.
Morris, M. D., & Bienstock, R. J. (1986) in *Spectroscopy of Biological Systems* (Clark, R. J. H., & Hester, R. E., Eds.) Vol. 13, pp 395–442, Wiley, Chichester, U.K.
Müller, F. (1981) *Photochem. Photobiol. 34*, 753–759.
Müller, F., Vervoort, J., Lee, J., Horowitz, M., & Carreira, L. A. (1983) *J. Raman Spectrosc. 14*, 106–117.
Nishimura, Y., & Tsuboi, M. (1978) *Chem. Phys. Lett. 59*, 210–213.
Nishina, Y., Kitagawa, T., Shiga, K., Horiike, K., Matsumura, Y., Watari, H., & Yamano, T. (1978) *J. Biochem. 84*, 925–932.
Nishina, Y., Shiga, K., Horiike, K., Tojo, H., Kasai, S., Yanase, K., Matsui, K., Watari, H., & Yamano, T. (1980) *J. Biochem. 88*, 403–409.
Pajot, P., & Groudinsky, O. (1970) *Eur. J. Biochem. 12*, 158–164.
Pajot, P., & Claisse, M. (1974) *Eur. J. Biochem. 49*, 275–285.
Parthasarathi, N., Hansen, C., Yamaguchi, S., & Spiro, T. G. (1987) *J. Am. Chem. Soc. 109*, 3865–3871.
Platenkamp, R. J., Palmer, M. H., & Visser, A. J. W. G. (1987) *Eur. Biophys. J. 14*, 393–402.
Prats, M. (1977) *Biochimie 59*, 621–626.
Reid, L. S., Lim, A. R., & Mauk, A. G. (1986) *J. Am. Chem. Soc. 108*, 8197–8201.

Scheidt, W. R., & Gouterman, M. (1983) in *Iron Porphyrins* (Lever, A. B. P., & Gray, H. B., Eds.) Part I, pp 89–139, Addison-Wesley, London.
Schejter, A., Glauser, S. C., George, P., & Morgoliash, E. (1963) *Biochim. Biophys. Acta 73*, 641–643.
Schmidt, J., Coudron, P., Thompson, A. W., Watters, K. L., & Mc Farland, J. T. (1983) *Biochemistry 22*, 76–84.
Schulz, G. E., Schirmer, R. H., & Pai, E. F. (1982) *J. Mol. Biol. 160*, 287–308.
Silvestrini, M. C., Brunori, M., Tegoni, M., Gervais, M., & Labeyrie, F. (1986) *Eur. J. Biochem. 161*, 465–472.
Spiro, T. G. (1985) *Adv. Protein Chem. 37*, 111–159.
Sugiyama, T., Nisimoto, Y., Mason, H. S., & Loehr, T. M. (1985) *Biochemistry 24*, 3012–3019.
Takano, T., & Dickerson, R. E. (1982) in *Electron Transport and Oxygen Utilization* (Ho, C., Ed.) pp 17–26, Macmillan Press, London.
Tegoni, M., Mozzarelli, A., Rossi, G. L., & Labeyrie, F. (1983) *J. Biol. Chem. 258*, 5424–5427.
Thomas, M.-A., Gervais, M., Favaudon, V., & Valat, P. (1983) *Eur. J. Biochem. 135*, 577–581.
Tsubaki, M., Nagai, K., & Kitagawa, T. (1980) *Biochemistry 19*, 379–385.
Vervoort, J., Müller, F., Le Gall, J., Bacher, A., & Sedlmaier, H. (1985) *Eur. J. Biochem. 151*, 49–57.
Vervoort, J., Müller, F., O'Kane, D. J., Lee, J., & Bacher, A. (1986) *Biochemistry 25*, 8067–8075.
Visser, A. J. W. G., Vervoort, J., O'Kane, D. J., Lee, J., & Carreira, L. A. (1983) *Eur. J. Biochem. 131*, 639–645.
Watari, H., Groudinsky, O., & Labeyrie, F. (1967) *Biochim. Biophys. Acta 131*, 592–594.
Watenpaugh, K. D., Sieker, L. C., & Jensen, L. H. (1973) *Proc. Natl. Acad. Sci. U.S.A. 70*, 3857–3860.
Wierenga, R. K., de Jong, R. T., Kalk, K. H., Hol, W. G. J., & Drenth, J. (1979) *J. Mol. Biol. 131*, 55–73.
Xia, Z.-X., Shamala, N., Bethge, P. H., Lim, L. W., Bellamy, H. D., Xuong, N. H., Lederer, F., & Mathews, F. S. (1987) *Proc. Natl. Acad. Sci. U.S.A. 84*, 2629–2633.

Raman/Absorption Simultaneous Measurements for Cytochrome Oxidase Compound A at Room Temperature with a Novel Flow Apparatus†

Takashi Ogura,‡ Shinya Yoshikawa,§ and Teizo Kitagawa*,‡

Institute for Molecular Science, Okazaki National Research Institutes, Myodaiji, Okazaki 444, Japan, and Institute for Basic Technology, Himeji Institute of Technology, Himeji 671-22, Japan

Received March 7, 1989; Revised Manuscript Received June 12, 1989

ABSTRACT: A novel flow apparatus for continuously producing reaction intermediates of cytochrome oxidase was constructed and applied successfully to observe the transient absorption and resonance Raman spectra in its reaction with oxygen. Time-resolved difference absorption spectra in 500–650-nm region clearly indicated the formation of compound A upon photolysis of the fully reduced CO-bound form at 5 °C, and at this stage electrons were not transferred from cytochrome *c* to cytochrome oxidase. However, at the stage of formation of compound B, cytochrome *c* was oxidized. Resonance Raman spectra of these intermediates measured simultaneously with the absorption spectra are also reported.

Cytochrome oxidase (EC 1.9.3.1) is the terminal enzyme in a respiratory chain of aerobic organisms. This enzyme catalyzes reduction of dioxygen coupled with vectorial proton translocation across the membrane (Wikström et al., 1981), and the resultant electrochemical potential is utilized by the H^+-ATPase to phosphorylate ADP. Mammalian cytochrome oxidases possess two heme A groups and two copper atoms per M_r = ~200 000, which are usually grouped into two functional units, namely, cytochromes *a* and a_3. Oxidized cytochrome *a* has a six-coordinated low-spin heme A and an EPR[1]-active copper atom, whereas cytochrome a_3 in the resting oxidized state has a high-spin heme A and an EPR-silent copper atom. Cytochrome *a* accepts electrons from cytochrome *c* and transfers them to cytochrome a_3. Cytochrome a_3 serves as the catalytic site for dioxygen reduction, but its mechanism still remains to be clarified. Since the reduced cytochrome oxidase reacts with O_2 very rapidly at physiological temperature, the conventional stopped-flow method with a few milliseconds of dead time after mixing is too slow to monitor the oxygenated reaction intermediates.

Cytochrome oxidase has a characteristic feature that its reduced form yields an adduct with carbonmonoxide (aa_3CO) which is photodissociable but otherwise stable. A lifetime of this adduct is about 30 s provided that it is mixed with O_2 in the dark. However, when the mixed solution is exposed to a flash of light, CO is photodissociated promptly and O_2 reacts with the photodissociated enzyme. The reaction kinetics involved were analyzed by monitoring the successive changes of absorption spectra after photolysis (Greenwood & Gibson, 1967; Orii, 1984; Blair et al., 1985). There have been arguments about whether the primary intermediate, compound A, which is characterized by absorption at 590 nm, is formed from the fully reduced enzyme at room temperature or not (Hill

† This work was supported by Grant-in-Aid for Scientific Research on Priority Areas 63617515 from the Ministry of Education, Science and Culture to T.K.

* Author to whom correspondence should be addressed.
‡ Institute for Molecular Science.
§ Institute for Basic Technology.

[1] Abbreviations: RR, resonance Raman; EPR, electron paramagnetic resonance.

0006-2960/89/0428-8022$01.50/0